Study of the Isothermal Transformation of Ductile Iron with 0.5% Cu by Electrical Resistance Measurement

B.Y. Lin, E.T. Chen, and T.S. Lei

A computer-controlled system for measuring electrical resistance has been developed and used to study the isothermal transformation of austenite in a ductile iron (3.31% C, 3.12% Si, 0.22% Mn, 0.55% Cu). The ability of the technique to follow the isothermal decomposition of austenite was established by measurements on an AISI 4340 steel. The times at which the austenite decomposed to primary ferrite, pearlite, and bainite were accurately detected. In the ductile iron, the formation of pearlite and of bainite was easily detected, and an isothermal transformation diagram was constructed from the results. The temperature range for the formation of bainite is especially important in producing austempered ductile iron (ADI) and was mapped. An initial stage of decomposition of austenite to ferrite and high-carbon austenite is followed by a time delay; then the high-carbon austenite decomposes to bainite. The formation of ADI requires austempering to a structure of ferrite and high-carbon austenite, then quenching to retain this structure, thus avoiding the formation of bainite. This is achieved by isothermal transformation into the time-delay region. For the ductile iron studied here, this time region was about 2.6 h at 400 °C and increased to 277 h at 300 °C.

Keywords

computer-controlled, ductile iron, electrical resistance, isothermal transformation

1. Introduction

DURING the isothermal transformation of ductile iron, austenite has two important modes of diffusional decomposition: eutectoid and bainite reactions. The eutectoid reaction of austenite in ductile iron is known to proceed by the metastable $\gamma \rightarrow \alpha + Fe_3C$ reaction, which results in the formation of pearlite, or by the stable $\gamma \rightarrow \alpha$ + graphite reaction, which forms ferrite and graphite. In addition, the metastable cementite constituent of pearlite can decompose to graphite and free ferrite: $Fe_3C \rightarrow \alpha$ + graphite. The competition between metastable and stable reactions is governed by the cooling rate of the casting and the composition of the ductile iron (Ref 1, 2).

The bainite reaction in ductile irons or in high-silicon steels is quite different from the bainite reaction that takes place in most low-silicon steels. During isothermal holding in the bainite-formation temperature range, the following two stages of reaction will occur. In the first stage, the austenite quenched from high temperature will decompose into ferrite and high-carbon austenite: $\gamma \rightarrow \alpha + \gamma_{hc}$. In the second stage, the high-carbon austenite will eventually decompose to ferrite and carbide: $\gamma_{hc} \rightarrow \alpha$ + carbide (Ref 3-5).

The first stage of bainite reaction produces a microstructure of acicular ferrite and carbon-rich austenite. Because austenite provides excellent ductility and ferrite provides good strength, the ductile iron has outstanding mechanical properties (Ref 6, 7). If the isothermal transformation is extended, with the reaction coming to the second stage, the carbon-rich austenite will finally decompose to ferrite and carbide. The second-stage reaction is undesirable, resulting in reduced ductility and toughness (Ref 8).

Austempered ductile iron (ADI) is a ductile iron that is treated by an isothermal heat treatment, called austempering, in the approximate range of 300 to 400 °C. This material has dramatically improved mechanical properties, due primarily to the mixture of fine bainitic ferrite and carbon-rich austenite present in the microstructure. Many investigators have studied the effects of metallurgical variables on the kinetics of austempering using various experimental techniques, such as hardness tests, quantitative metallography (Ref 9, 10), magnetic change (Ref 11), dilatometry (Ref 11, 12), x-ray diffraction (Ref 8, 13), and resistivity measurement (Ref 14), to measure the phase transformation. However, many aspects related to the response of isothermal treatment require further examination.

In this investigation, a vacuum heat treating system controlled using a personal computer (PC) was developed and used to

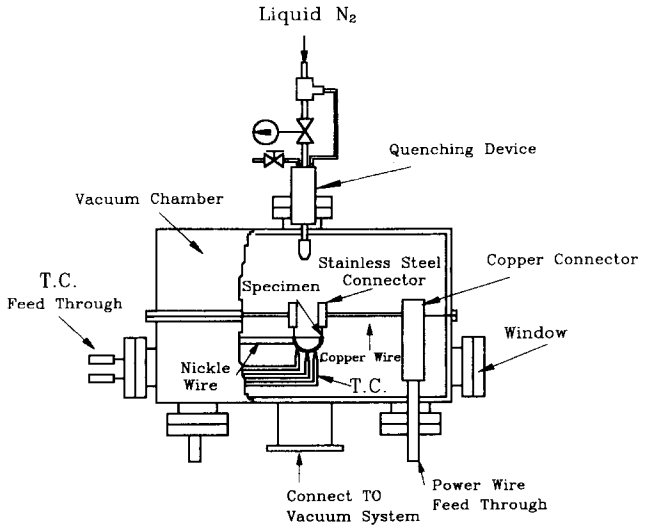

Fig. 1 Schematic drawing of the vacuum furnace and specimen arrangement

B.Y. Lin, E.T. Chen, and **T.S. Lei,** Department of Mechanical Engineering and Technology, National Taiwan Institute of Technology, Taipei, Taiwan 10722, Republic of China

measure electrical resistance during the isothermal transformation process. Essentially, this system provides a continuous measuring technique that allows investigation of the kinetics of phase transformation through resistance changes. It is also very convenient for conducting several simultaneous isothermal heat treatments using a single specimen. The resulting resistance data for isothermal reactions were used to construst a partial isothermal transformation (IT) diagram for a ductile iron containing 0.5% Cu.

2. Experimental Procedure

2.1 *Equipment Setup and Measurement Accuracy*

A PC-controlled vacuum heat-treating device combined with a system for measuring electrical resistance was used to study the isothermal phase transformation of ductile iron. Figure 1 shows a schematic drawing of the vacuum furnace and specimen. The specimen, 3 mm in diameter and 100 mm long, was heated via direct current (dc) to the austenitizing temperature, quenched with a spray of liquid nitrogen to a lower temperature, and then its temperature controlled at a desired isothermal level. The resistance during isothermal transformation was measured by the four-wire method with a 5½-digit voltmeter (HP3478A, resolution of 100 nV) and a dc power supply (HP6031A, accuracy of 0.25%) via a real-time scheme. The temperature of the specimen was measured by three pairs of K-type thermocouples that were connected through thermocouple transmitters and an analog-to-digital/digital-to-analog (AD/DA) converter (resolution of 14 bits) to a personal computer. The thermocouple voltage was read by a thermocouple measuring and calibration unit (Linseis T-DLIN-C, resolution of 10 μV). The accuracy was ±1 °C. The hardware and software of this system have been illustrated in great detail in recent reports (Ref 15, 16).

In this experiment, the temperature oscillation has been limited in the early stage by tuning the time constants of a proportional integral derivative (PID) model algorithm in the control program. As shown in Fig. 2, both temperature curves oscillate in the initial 40 s with an amplitude of around ±10 °C. After 40 s, the temperature is kept essentially constant with a fluctuation within ±1 °C.

An AISI 4340 steel (0.36C-0.81Mn-0.2Si-0.8Cr-1.7Ni-0.17Mo) was chosen for testing the accuracy of the experimental equipment. Figure 2 presents two pairs of temperature and resistance records of a 4340 steel specimen that was isothermally treated at 600 and 370 °C in the vacuum furnace after quenching from 850 °C. Both temperature curves oscillate initially with an amplitude of around ±10 °C for about 40 s. Later, the mean temperature of the specimen is maintained within ±1 °C for the isothermal treatment. The resistance curve at 370 °C shows that the resistance is approximately constant, even though the temperature shows a little oscillation during the initial progress. Then the resistance curve starts to decrease rapidly after 25 s, indicating the start of bainite formation (B_s) and levels off after about 500 s, indicating the finish of the transformation (B_f). The curve represents the transformation of austenite to bainite (Ref 17). At 600 °C the curve has a slow decline after 30 s (F_s), which should be due to the ferrite nucleating and growing in the austenite. The resistance then decreases rapidly after 700 s (P_s) and levels off after 7000 s (P_f)—the start and finish, respectively, of pearlite formation. This resistance curve represents the transformation of austenite to ferrite and pearlite (Ref 17).

Figure 3 shows the resistance records obtained during isothermal holding of 4340 specimens at 320, 370, 420, 470, 540, 600, 650, and 680 °C. From these curves, the progress of austenite decomposition was determined and the partial IT diagram constructed, as shown in Fig. 4. The IT diagram of 4340 steel published in Ref 18 is shown in Fig. 5. A comparison of Fig. 4 and 5 shows that both match quite well. The pearlite and bainite reactions in Fig. 4 are faster than those in Fig. 5. This could be due to the difference in the austenite grain size. The grain size of austenite in Fig. 5 ranged from ASTM No. 7 to No. 8. A special etching technique (Ref 19) revealed that the grain size of austenite for the 4340 steel studied here (after austenitizing at 850 °C for 20 min) was around ASTM No. 9. For a smaller grain size with a lower hardenability, the time of the phase transformation will be lower. Therefore, the results of Fig. 4 should be considered as reasonable and confirm both the sensitivity and the accuracy of this experimental system.

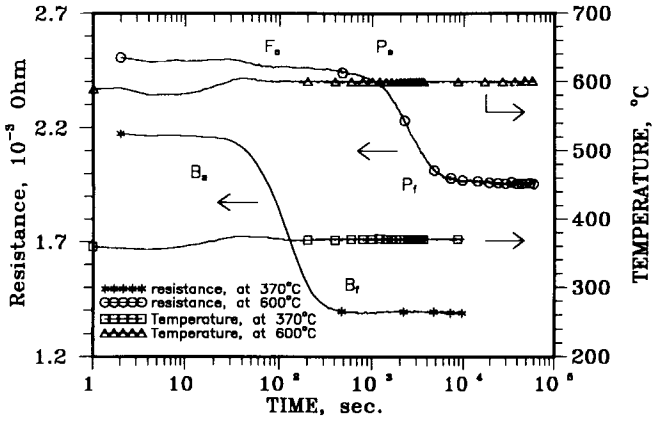

Fig. 2 Temperature and resistance records of AISI 4340 steel isothermally treated at 370 and 600 °C

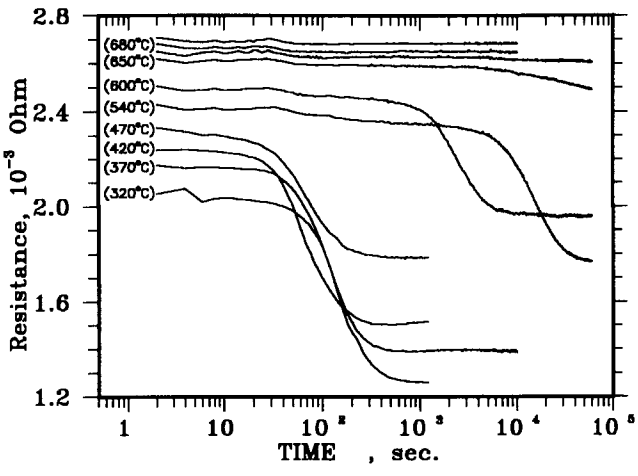

Fig. 3 Resistance records of AISI 4340 steel during isothermal transformation at various temperatures

2.2 *Experimental Procedure*

The chemical analysis in weight percent of the experimental ductile iron heat was 3.31C-3.12Si-0.22Mn-0.03P-0.01S-0.02Mg-0.55Cu. This heat was prepared in a high-frequency induction melting furnace using charges composed of pig iron, steel scrap, ferrosilicon, ferromanganese, and pure copper. The melt was heated to around 1530 °C, then was treated using the sandwich technique and poured into a graphite pipe mold at approximately 1430 °C. The specimens, 3 mm in diameter and 100 mm long, were obtained directly from the graphite pipe mold. Their surfaces were smooth enough that no machining was required.

The specimens were placed in the furnace of the vacuum heat-treating system, austenitized at 900 °C for 1 h, then quenched to desired transformation temperatures of 300, 350, 380, 400, 430, 460, 500, 600, 650, and 700 °C. The temperature and the resistance of the specimens were measured during the progress of isothermal holding. The resistance data were used to construct an IT diagram for the ductile iron.

In order to substantiate the resulting IT diagram, a metallographical examination was conducted. Four specimens were sectioned from a bar 3 mm in diameter and 100 mm long. They were then austenitized at 900 °C in a salt bath for 1 h, followed by a quench and isothermal hold for 20 min in a salt bath at 300, 400, 500, and 550 °C, respectively. The resulting microstructures of the specimens were examined in a scanning electron microscope and an optical microscope.

3. Results and Discussion

3.1 *Relation between Resistance Change and the Isothermal Transformation of Ductile Iron*

The microstructure of ductile iron includes nodular graphite and a high-silicon, high-carbon iron-base matrix. During the progress of isothermal holding, the nodular graphite and its relative contents will remain unchanged; therefore, its effect on resistivity can be neglected. The high-silicon, high-carbon iron-base matrix, however, will undergo complicated phase transformations during the isothermal treatment, and their effect on resistance will change with time.

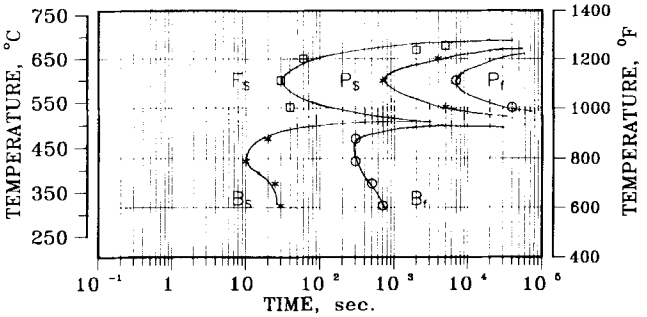

Fig. 4 AISI 4340 IT diagram, constructed from resistance measurements. Composition: 0.36C-0.81Mn-0.2Si-0.8Cr-1.78Ni-0.17Mo. Austenitized at 850 °C for 20 min. Grain size: ASTM No. 9

Figure 6 presents the resistance records of the ductile iron during isothermal treatment at various temperatures. The curve of 400 °C, located in the upper bainite reaction temperature region, shows that the resistance started to decrease after 30 s and leveled off around 700 s. This progress from 30 to 700 s should be the first stage of bainite reaction ($\gamma \rightarrow \alpha + \gamma_{hc}$). Then the resistance started to decline distinctly again at around 10,000 s, indicating the onset of the second stage of the bainite reaction; in other words, the austenite began to decompose to ferrite and carbide ($\gamma_{hc} \rightarrow \alpha$ + carbide). At about 60,000 s, the curve was gradually reaching another stable value, which could mean that the high-carbon austenite in the matrix was almost exhausted, indicating that the second stage of bainite reaction was also approaching completion.

The resistance at 600 °C, which should be located in the eutectoid transformation temperature range, decreased rapidly at about 10 s and became smooth at around 30 s, indicating the start and finish of the eutectoid reaction (the metastable $\gamma \rightarrow \alpha + Fe_3C$ or the stable $\gamma \rightarrow \alpha$ + graphite). Unfortunately, the resistance records do not allow the stable and the metastable eutectoid reactions to be distinguished.

Comparison of all the resistance curves in Fig. 6 shows that there is no clear turning point in the 700 °C curve, indicating that no phase transformation occurred during the isothermal holding. At about 650 and 500 °C, the curves, like the curve at 600 °C, declined and became smooth just one time, indicating that only the eutectoid reaction occurred. The 460, 430, 380, 350, and 300 °C curves are similar to the curve at 400 °C, located in the bainite reaction temperature range, and the resistance of those curves should have two changes during the isothermal progress. However, it is seen that the second reaction time in 460 and 430 °C curves is shorter than that in 400 °C and in 380, 350, and 300 °C curves is much longer than in 400 °C, so that the curves at 350 and 300 °C only show the first stage reaction.

3.2 *Isothermal Transformation Diagram*

The turning points of all the curves in Fig. 6 are taken as the start and finish times of the phase transformations and are listed in Table 1. Figure 7 shows the IT diagram of the ductile iron, which was constructed using the data in Table 1.

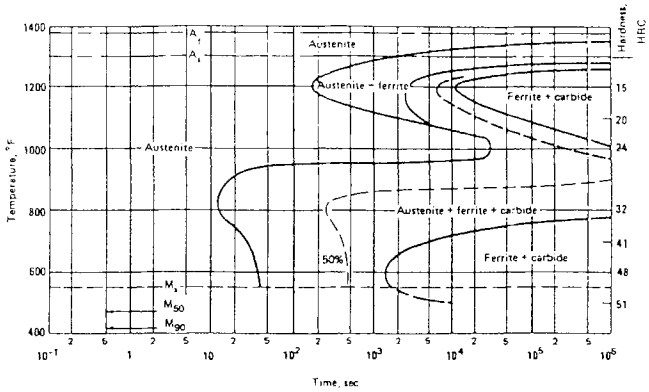

Fig. 5 AISI 4340 IT diagram reported in Ref 18. Composition: 0.42C-0.78Mn-1.79Ni-0.8Cr-0.33Mo. Austenitized at 845 °C. Grain size: ASTM No. 7 to No. 8

Table 1 Starting and finishing phase transformation times of all curves in Fig. 6

Temperature, °C	Start of eutectoid reaction (E_s), s	Finish of eutectoid reaction (E_f), s	Start of first-stage bainite reaction ($B1_s$), s	Finish of first-stage bainite reaction ($B1_f$), s	Start of second-stage bainite reaction ($B2_s$), s	Finish of second-stage bainite reaction ($B2_f$), s
700	...	...	...	...	...	...
650	20	40	...	...	...	...
600	10	30	...	...	...	...
500	50	500	...	...	...	...
460	...	...	20	200	700	2,000
430	...	...	20	400	2,000	7,000
400	...	...	30	700	10,000	60,000
380	...	...	40	900	200,000	...
350	...	...	50	1,200	...	...
300	...	...	100	2,000	...	...

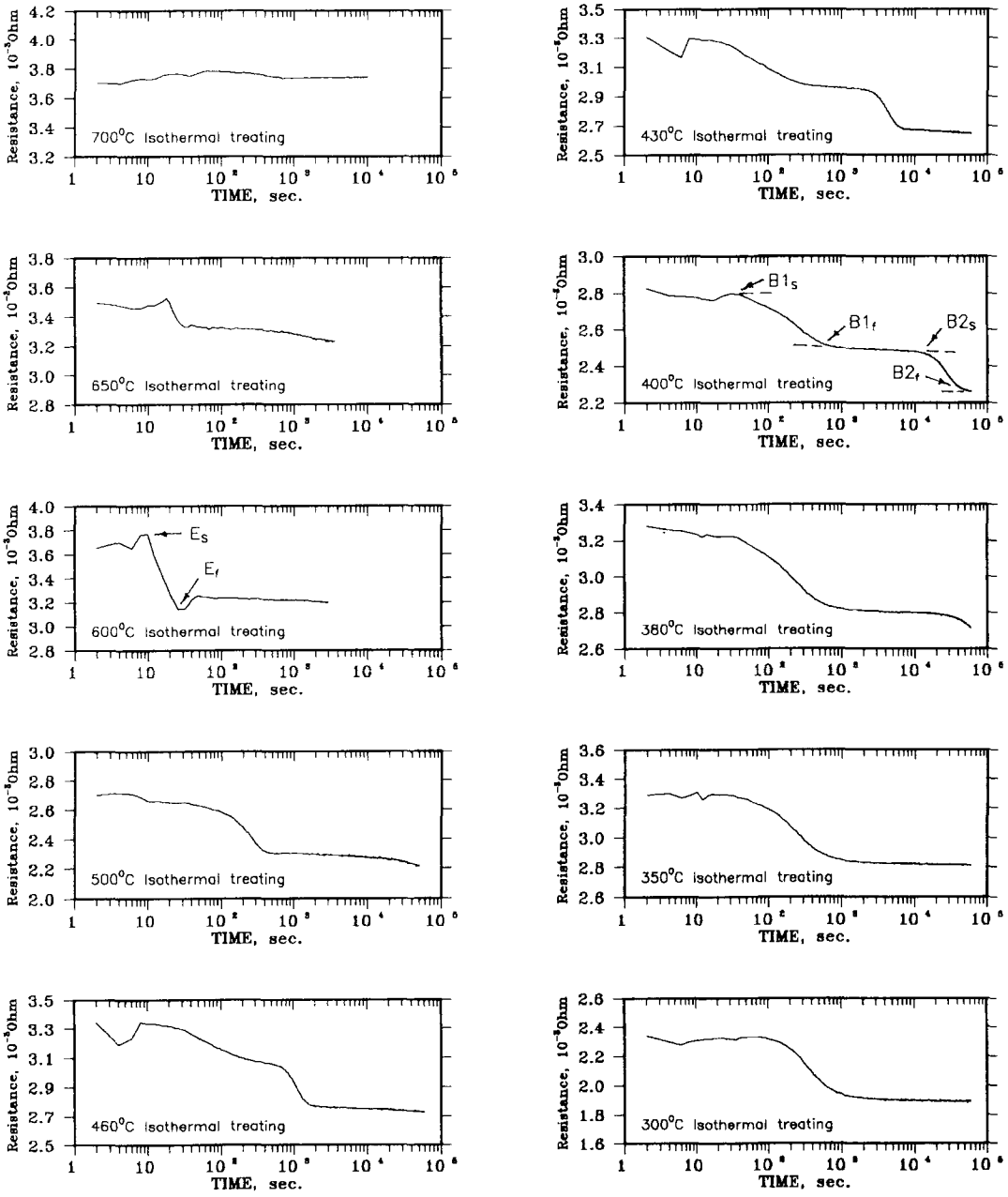

Fig. 6 Resistance records of the ductile iron during isothermal transformation at various temperatures

It is obvious from Fig. 7 that the bainite formation range of approximately 300 to 450 °C is different from that of most steels. There are two pairs of reaction lines: the $B1_s$ and $B1_f$ lines, illustrating the start and finish times, respectively, of the first-stage reaction; and the $B2_s$ and $B2_f$ lines, representing the start and finish, respectively, of the second-stage reaction. The area between the $B1_f$ and $B2_s$ lines gives a significant window of time (Ref 4, 8, 14), Δt_i, during which the maximum amount of high-carbon austenite is present and the optimum mechanical properties can be obtained. Thus, the type of IT diagram shown in Fig. 7 is very useful for austempering ductile iron to select the parameters for heat treatment. However, previous reports about the IT diagram (Ref 9, 10, 20) rarely illustrated the second stages of bainite transformation completely. High-quality ADI requires establishing a series of complete IT diagrams of ductile iron that contain B1 and B2 reaction lines.

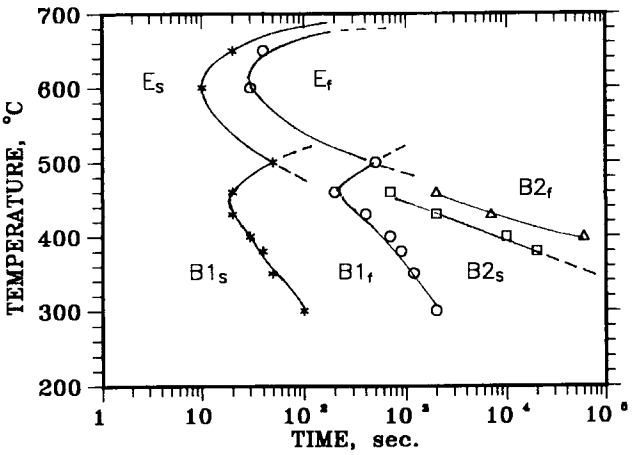

Fig. 7 Isothermal transformation diagram of the ductile iron (3.3C-3.12Si-0.22Mn-0.55Cu) austenitized at 900 °C for 1 h

Figures 8(a) to (d) illustrate the microstructures of the ductile iron after austenitizing for 1 h at 900 °C and isothermal treatment for 20 min at 300, 400, 500, and 550 °C, respectively. Figures 8(a) and (b) show the lower and upper bainite structures, in which the matrix consists of plates of acicular ferrite in carbon-rich austenite, indicating that the first bainite reaction is already accomplished. Figures 8(c) and (d) show the carbide and ferrite mixed structures only (no martensite), indicating that the eutectoid reaction is also completed. The IT diagram of

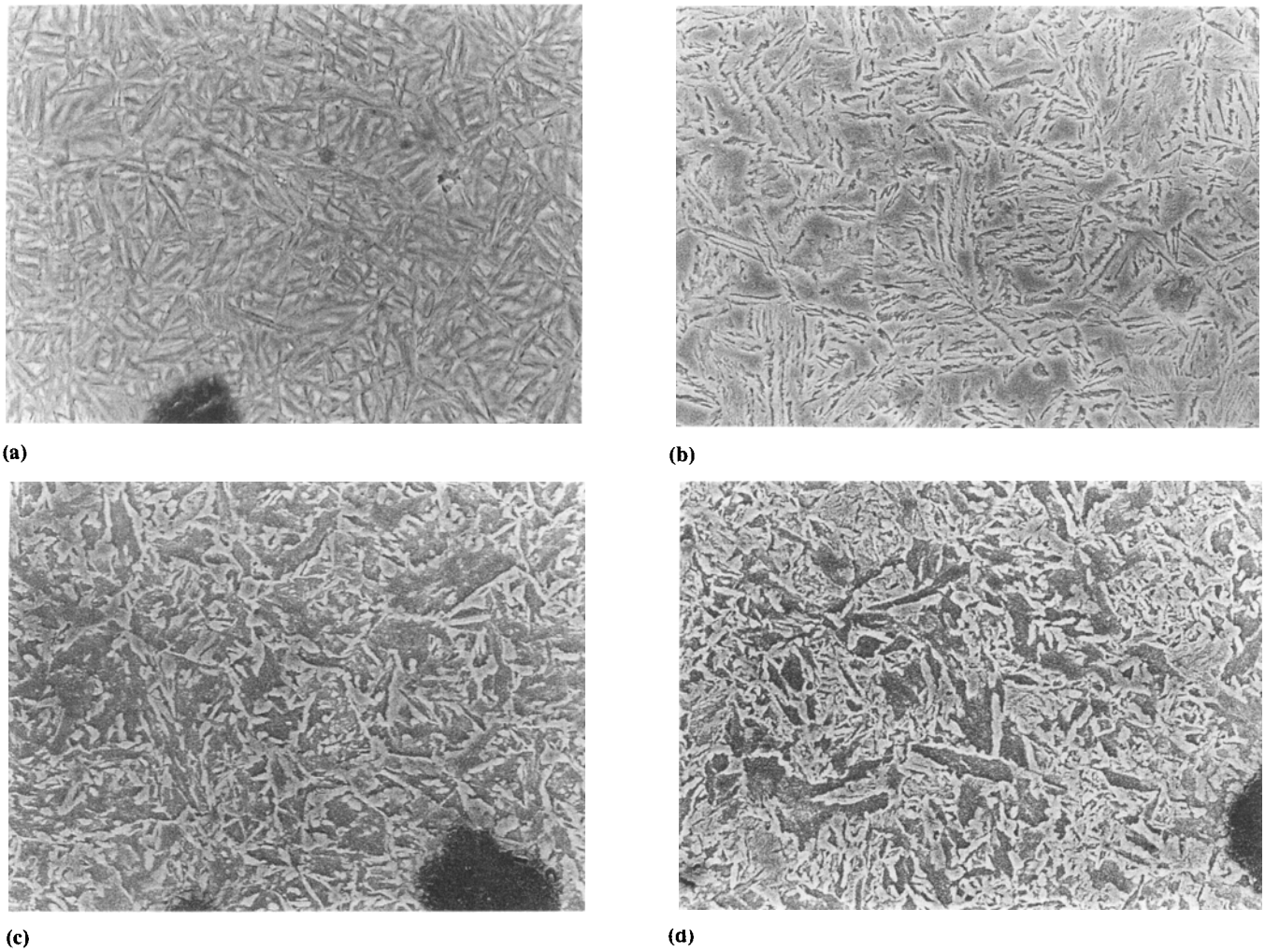

Fig. 8 Microstructures of ductile iron with 0.5% Cu, austenitized for 1 h at 900 °C and isothermally treated for 20 min at (a) 300 °C, (b) 400 °C, (c) 500 °C, and (d) 550 °C

the ductile iron shown in Fig. 7 indicates that at 1200 s at all temperatures both the eutectoid reaction and the first stage of bainite reaction have been accomplished. This result is in conformance with the microstructures in Fig. 8, indicating that the resistance-measuring method of this experiment is quite useful for determining the IT diagram of ductile iron.

3.3 *Relation between Δt_i and Austempering Time*

Many investigators (Ref 4, 8, 14) have demonstrated that the time, Δt_i, separating the two stages of ADI during bainite transformation is affected by many factors, including austenitizing temperature, austempering temperature, isothermal holding time, alloying elements, and segregation. However, these effects rarely have been reported with a quantitative method.

The $B1_f$ and $B2_s$ lines, redrawn from Fig. 7, are shown in Fig. 9. It can be seen that both the $B1_f$ and the $B2_s$ times are delayed significantly at low austempering temperatures. The area between the $B1_f$ and $B2_s$ lines is also greatly affected by austempering temperature. It is very narrow within the upper temperature range, but becomes wider when the temperature decreases. The separating time, Δt_i, is only about 2.6 h at 400 °C and around 27 h at 350 °C, but dramatically increases to 277 h at 300 °C. Thus, it can be seen that obtaining optimum mechanical properties of ADI, which requires a maximum amount of carbon-rich austenite, may not be difficult using the lower austempering temperature.

4. Conclusions

Measurement of electrical resistance was used to study the isothermal transformation of ductile iron. Both the eutectoid reaction and the first and second stages of bainite reaction were easily detected.

An IT diagram of a specific ductile iron was constructed based on the resistance data obtained. The diagram contained two pairs of transformation lines within the austempering temperature range and proved useful in selecting the austempering time for ADI.

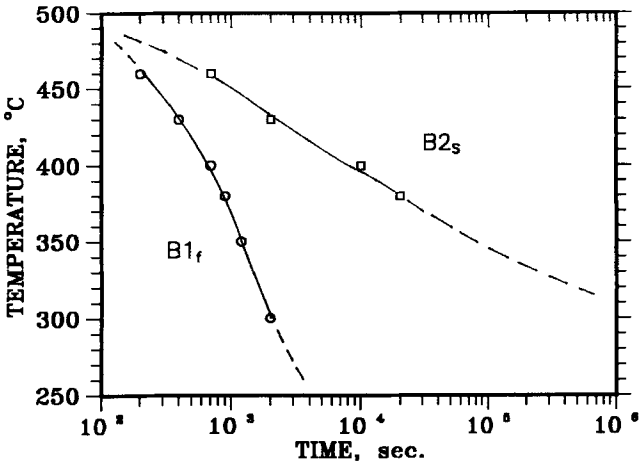

Fig. 9 The first reaction finishing line, $B1_f$, and the second reaction starting line, $B2_s$, as a function of austempering time for the 0.5% Cu ductile iron

The time window, Δt_i, is greatly affected by the austempering temperature. It is short in the upper temperature range, but very long in the lower temperature range. It appears that obtaining a maximum amount of carbon-rich austenite in the lower austempering temperature range for ADI is not difficult.

Acknowledgments

The authors would like to thank Prof. Charlie R. Brooks for reading and commenting on this paper. We also are grateful for the partial financial support of this work by the National Science Council of the Republic of China under grant No. NSC 80-0405-E011-08.

References

1. W.C. Johnson and B.V. Kovacs, The Effect of Additives on Eutectoid Transformation of Ductile Iron, *Metall. Trans. A*, Vol 9A, 1978, p 219-229
2. E.M. Pan, M.S. Lou, and C.R. Loper, Jr., Effects of Copper, Tin, and Manganese on the Eutectoid Transformation of Graphite Cast Irons, *AFS Trans.*, Vol 95, 1987, p 819-840
3. P.A. Blackmore and R.A. Harding, The Effect of Metallurgical Process Variables on the Properties of Austempered Ductile Iron, *J. Heat Treat.*, Vol 3 (No. 4), 1984, p 310-325
4. J.F. Janowak and R.B. Gundlach, Development of A Ductile Iron for Commercial Austempering, *AFS Trans.*, Vol 91, 1983, p 377-388
5. R.C. Voigt, Microstructural Analysis of Austempered Ductile Cast Iron Using the Scanning Electron Microscope, *AFS Trans.*, Vol 91, 1983, p 253-262
6. M. Johansson, Austenitic-Bainitic Ductile Iron, *AFS Trans.*, Vol 85, 1977, p. 117-122
7. D.J. Moore, T.N. Rounds, and K.B. Rundman, The Effect of Heat Treatment, Mechanical Deformation and Alloying Element Additions on the Rate of Bainite Formation in Austempered Ductile Iron, *J. Heat Treat.*, Vol 4 (No. 1), 1985, p 7-24
8. D.J. Moore, T.N. Rounds, and K.B. Rundman, Structure and Mechanical Properties of Austempering Ductile Iron, *AFS Trans.*, Vol 93, 1985, p 705-718
9. D.J. Moore, B.S. Shugart, K.L. Hayryne, and K.B. Rundman, A Microstructure Determination of Isothermal Transformation Diagram in a Low-Alloy Ductile Iron, *AFS Trans.*, Vol 98, 1990, p 519-526
10. D.J. Moore, G.P. Faubert, E.D. McCarty, D.J. Ellerbrock, and K.B. Rundman, Isothermal Transformation Diagram in a Heavy-Section, High-Alloy Ductile Cast Iron, *AFS Trans.*, Vol 98, 1990, p 449-457
11. K. Yasue, T. Nisio, Y. Yamada, and Y. Obata, Effects of Alloying Elements and Austenitizing Conditions on the Isothermal Transformation Diagram of Ductile Cast Iron, *Imono (J. Jpn. Foundrymen's Soc.)*, Vol 63, Dec 1991, p 595-600
12. J.P. Chobaut, P. Brenot, and J.M. Schissler, Secondary Martensite Formation during the Tempering of Bainite S. G. Cast Iron, *AFS Trans.*, Vol 96, 1988, p 475-480
13. B.Y. Lin, "A Study on Austemperability of Ductile Iron," Master's thesis, National Taiwan Institute of Technology, 1987
14. Y.J. Park, R.B. Gundlach, and J.F. Janowark, Monitoring the Bainite Reaction during Austempering of Ductile Steel by Resistivity Measurement, *AFS Trans.*, Vol 95, 1987, p 411-416
15. B.Y. Lin, E.T. Chen, and T.S. Lei, "The Use of Electrical Conductivity on the Study of the Austemperability of Ductile Irons," NSC 80-0405-E011-08, National Science Council, Taipei, Taiwan, Republic of China, 1991

16. B.Y. Lin, E.T. Chen, and T.S. Lei, The Use of Electrical Conductivity on the Study of the Austemperability of Ductile Irons, *Proc. 1992 Ann. Conf. Chinese Society for Materials Science*, H.K. Wu, Ed., Chinese Society for Materials Science, Taipei, Taiwan, Republic of China, 1992, p 44

17. G.T. Eldis, A Critical Review of Data Source for Isothermal Transformation and Continuous Cooling Transformation Diagram, *Hardenability Concepts with Application to Steel*, D.V. Doane and J.S. Kirkaldy, Ed., Metallurgical Society of AIME, 1978, p 126-148

18. P.M. Unterweiser, H.E. Boyer, and J.J. Kubbs, *Heat Treater's Guide: Standard Practices and Procedures for Steel*, American Society for Metals, 1982, p 161

19. G. Krauss, *Principles of Heat Treatment of Steel*, American Society for Metals, 1980, p 172

20. K. Röhrig and W. Fairhust, *Die Wärmebehandlung des Gusseisens mit Kugelgraphit und die Umwandlungsschaubilder*, No.6, Deutscher Giesserei Verband, Dusseldorf, 1979